Scanning Electron Microscopy

Volume 1985 | Number 3 Article 11

8-9-1985

# A High Efficiency Cathodoluminescence System and its Application to Optical Materials

A. D. Trigg
*Hirst Research Centre*

SCANNING ELECTRON MICROSCOPY/1985/III (Pages 1011-1022)
SEM Inc., AMF O'Hare (Chicago), IL 60666-0507 USA

0586-5581/85$1.00+.05

# A HIGH EFFICIENCY CATHODOLUMINESCENCE SYSTEM AND ITS APPLICATION TO OPTICAL MATERIALS

A D Trigg*

GEC Research Limited, Hirst Research Centre, East Lane, Wembley, HA9 7PP, UK

(Paper received February 28, 1985: manuscript received August 09, 1985)

## Abstract

A high collection efficiency spectroscopic cathodoluminescence (CL) system based on an in-line ellipsoidal mirror has been constructed for use on a Cambridge S250 scanning electron microscope (SEM). It can be fitted to or removed from the SEM in about 30 minutes and requires no significant modification of the instrument. It can be used to obtain total CL images, monochromatic CL images or CL spectra with an ultimate spectral resolution of 1 nm.

The system has been applied to the study of doped synthetic quartz crystals, optical fibres and optical fibre preforms, and to yttrium aluminium garnet, bismuth silicon oxide and potassium tantalum niobate crystals. The CL technique has proved particularly valuable in the study of quartz and has revealed a number of interesting features related to crystal growth. For optical fibres and their preforms CL provides a convenient method of monitoring the distribution of germanium, used as a dopant to increase the refractive index in the core region of the fibre.

KEY WORDS: cathodoluminescence, scanning electron microscope, spectroscopy, aluminium doped quartz, germanium doped quartz, optical fibre, bismuth silicon oxide, yttrium aluminium garnet, silica.

*Address for Correspondence:
A D Trigg
GEC Research Limited, Hirst Research Centre, East Lane, Wembley, Middlesex, HA9 7PP, UK

Phone No: (01) 904-1262

## Introduction

The cathodoluminescence (CL) mode of the scanning electron microscope (SEM) has been recognised for many years as a valuable technique for the study of semiconductors, organic compounds and a range of inorganic materials, particularly phosphors and natural minerals (Brocker and Pfefferkorn, 1978, 1980). However, it is probably only in the field of compound semiconductors that the technique has realised its full potential and been used widely on a routine basis. Despite its obvious relevance to other materials, such as phosphors and scintillators for example, it has not gained the widespread acceptance achieved by either the energy-dispersive X-ray analysis (EDX) or backscattered electron imaging (BSE) modes of the SEM, although it was first used before either of these techniques became widely available.

There appear to be two main, partially inter-related reasons for this situation. Firstly, interpretation of CL results, whether in the form of images or spectra, is far more complex than for either EDX or BSE. Whereas there is a simple relationship between the electron backscattering factor and mean atomic number or between X-ray peak energy and atomic number (Moseley's Law) no such simple interpretation of CL spectra can be given. Both electron backscattering and X-ray generation depend only on the atoms present in the solid; they are virtually insensitive to how these atoms are bound together. No such simplification exists for luminescence but while this creates problems in interpretation it also leads to the high sensitivity of CL to impurity levels and strain which is so valuable. For narrow ranges of materials such as III-V compound semiconductors the interpretation of CL is well advanced (see for example Holt and Datta, 1980, Lohnert and Kubalek, 1983). In general, however, interpretation is likely to remain difficult for some years to come.

In the absence of any general theoretical framework for relating CL spectra and images to materials properties, an empirical, ad-hoc approach is often required. This is hampered by the relatively few published results on materials other than semiconductors. Even in the field of high brightness phosphors for which SEM based CL

might appear to be the ideal technique for materials studies, surprisingly little has been reported (Richards et al, 1983).

Secondly, there are significant experimental difficulties in acquiring useful CL results. Total CL images can be obtained very easily on all SEMs simply by pointing a photomultiplier tube (PMT) at the specimen but the collection efficiency is low and interpretation of the image is very difficult in the absence of information on the CL emission wavelength(s). At the other end of the scale sophisticated high efficiency CL systems such as those described by Davidson and Rasul (1977) Holt et al (1976) Lohnert et al (1981) or Beavineau and Semo (1982) are expensive and require an SEM to be dedicated to CL studies. This is only rarely possible, especially in industrially oriented laboratories.

Outside the semiconductor field improvements in interpretation will be limited until more results are published and there is a greater general interest, while there is unlikely to be a high investment in dedicated CL systems until the results emanating from them can be confidently related to materials properties.

The aim of the present work has been to escape from the closed loop just described by developing a relatively low cost high efficiency versatile spectroscopic CL system which can be easily mounted on an existing standard SEM (Cambridge Instruments S250 MkII) as and when required. Because of the nature of the work in the author's laboratory it was essential that the CL system could be quickly demounted (in less than one hour) and the SEM returned to other tasks with no compromise of its normal functions.

The other requirements of the CL system were as follows: (1) As high a collection efficiency as possible so that materials with low CL output could be examined. (2) The ability to obtain total CL images, monochromatic CL images and CL spectra with an ultimate spectral resolution of ~1 nm. (3) Operation over the spectral range 300-800 nm initially but with the possibility of extension to 20 μm at a later date. (4) That the system could be subsequently modified to incorporate a cold stage capable of reducing the specimen temperature to less than 100K.

Once an outline specification had been established a limited survey was made of the various CL systems possible and their relative merits were assessed. The results of this survey are summarised in Table 1; it is by no means exhaustive. (For a full review of various types of CL detection system see Holt, 1981). It appeared that the most promising design was that described by Davidson et al (1976) (see also Davidson and Rasul, 1977). The specimen is located at the first focus of an ellipsoidal mirror having its major axis in line with the electron beam. Light emitted from the specimen is brought to focus at the second focus of the mirror which is arranged to be outside the specimen chamber by means of a plane mirror.

This approach appeared to offer some significant advantages over other ellipsoidal mirror systems in which the major axis is perpendicular to the electron beam direction. In particular, it is possible by appropriate choice of mirror geometry to achieve any desired degree of angular compression so that the output of the collection system can be matched to the acceptance angle of the monochromator without the need for any condenser lens. Since the second focus of the mirror is outside the vacuum system, alignment of the monochromator input slit with the focus is relatively simple. Another advantage is that, with the exception of the plane window at the vacuum-air interface, reflecting optical surfaces are used throughout and hence the collection system imposes no restrictions on the spectral range which may be covered. There are, however, some drawbacks to this approach. Alignment of the CL emission point with the first focus of the ellipsoidal mirror is critical, suitable ellipsoidal mirrors are not easily available commercially and, most importantly, there must be a clear space below the specimen where the plane mirror is placed. It is this last aspect which places severe restraints on the SEM specimen chamber and stage and in the system designed by Davidson et al this requirement could only be met by using a heavily modified SEM with a purpose built chamber and stage.

In the period since that system was built there has been a trend towards designing SEMs to accommodate much larger specimens, driven largely by the requirements of the semiconductor industry. The most recently acquired SEM in the author's laboratory, a Cambridge Instruments S250, has a specimen chamber whose internal dimensions are 210 mm x 260 mm x 190 mm and X and Y stage movements of ±50 mm. In addition, the tilt-rotation-height substage can be displaced by a further 35 mm. An initial feasibility study showed that there was sufficient space in the chamber to accommodate both the ellipsoidal mirror above the specimen and the plane mirror beneath it without any modification of either chamber or stage.

## The CL collection system

The most critical component of the system is the ellipsoidal mirror which is located immediately beneath, and co-axial with, the final lens of the SEM, see Figure 1. The mirror was

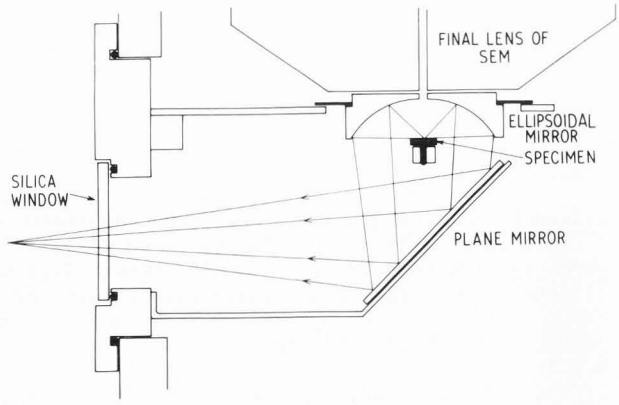


Figure 1 Diagram of CL collection system mounted in the SEM

Table 1 : Types of SEM based cathodoluminescence system.

| | CL System | Ease Of Interface To SEM | Collection Efficiency (approx)* | Wavelength Range | CL Spectra | Comments |
|---|---|---|---|---|---|---|
| 1 | Simple photomultiplier (PMT) | Good | 1% | Depends only on PMT | No | Cheap |
| 2 | PMT with collection lens | Good | 5% | Depends on lens | No | Commercially available for most SEMs |
| 3 | PMT with transparent light pipe | Good | 30% | Depends on light pipe | No | Commercially available for some SEMs |
| 4 | PMT with internally reflecting light pipe (Boyde and Reid 1983) | Good | 50% | Depends only on detector | No | |
| 5 | Solid state detector mounted close to sample (Chin et al 1984) | Fair | 30% | Depends on detector. Useful for IR | No | Backscattered electrons may interfere with signal |
| 6 | Systems 2-4 with optical filters | Fair | Depends on system | Depends on system | No | Can provide monochromatic images |
| 7 | Monochromator with collection lens | Fair | 5% | Depends on lens | Yes | Simplest method for spectroscopic CL |
| 8 | As 7 with fibre optic coupling | Fair | 5% | Depends on lens and fibre-optic | Yes | Profile of fibre-optic can be matched to input slit |
| 9 | Lateral ellipsoidal mirror with fibre-optic coupling (Hörl 1972) | Moderately difficult | 90% | Depends on fibre-optic | No | |
| 10 | As 9 with optical filters (Hörl 1978) | Moderately difficult | 90% | Depends on fibre-optic | Yes | Can provide monochromatic images |
| 11 | As 9 with condenser lens and monochromator (Steyn et al, 1976) (Carlsson and van Essen 1974) | Moderately difficult | ? | Depends on lens and fibre-optic | Yes | Available commercially Difficult to align |
| 12 | Lateral ellipsoidal mirror directly coupled to monochromator (Löhnert et al 1981) | Moderately difficult | 30% | Depends only on window | Yes | |
| 13 | In-line ellipsoidal mirror and monochromator (Davidson et al, 1976) | Difficult | 90% | Depends only on detector and window | Yes | |
| 14 | As 12 with interferometer instead of monochromator (Davidson et al 1981) | Difficult | 90% | As above | Yes | Offers significant advantages in IR region. Cannot provide monochromatic images |
| 15 | Dedicated spectrometer using parabolic mirror (Beauvineau and Semo 1982) | Compatible with Cameca SEM MEB07 | ? | 0.2 - 3.0 μm | Yes | |

* Maximum possible collection efficiency calculated assuming no losses at optical surfaces

designed so that the first focus is at 17 mm, giving a convenient working distance on the SEM of ~20 mm. The second focal length was chosen to be 300 mm, slightly longer than that used by Davidson et al so as to ensure that the second focus was well clear of the side of the SEM after reflection by the plane mirror. The diameter of the ellipsoidal mirror is 64 mm to give an optical aperture at the second focus of f/4.6, slightly less than the input aperture of the monochromator, f/4.

Once the optical parameters had been decided a two dimensional template was cut using a numerically controlled milling machine. From the template a three-dimensional brass convex former was machined using a pattern following lathe. After the former had been polished a concave epoxy mirror was cast from it, machined to the correct external dimensions and polished using successively smaller diamond paste down to 0.25 μm. Finally, it was aluminised by vacuum evaporation.

Because of the requirement for easy demountability the ellipsoidal mirror, plane mirror and optical window are all mounted on a plate fitting in the 125 mm diameter port on the left side of the chamber, see Figure 1. Accurate alignment of the axis of the ellipsoidal mirror with that of the SEM column is essential and hence the lateral position of the mirror is adjustable by ±3 mm in both X and Y directions. Once aligned it is clamped permanently in position. The plane mirror is also front aluminised and the window is an optically flat disc of high purity silica 5 mm thick. This thickness of silica is insufficient to provide X-ray shielding and hence a health hazard could arise, especially if a high electron beam current at 40 keV were to strike the plane mirror. An interlock system is therefore provided so that the electron gun high voltage supply will only operate if either a 10 mm thick lead glass window is in position outside the silica window or the monochromator is in position to prevent accidental X-ray exposure.

The need for a clear unobstructed light path beneath the specimen, and the presence of the plane mirror precludes the use of the standard stage in the normal manner. Instead the specimen, mounted either on a standard 12.5 mm diameter 'pin' stub or, for maximum collection efficiency, a smaller 8 mm diameter stub, is held at the end of a 50 mm long rod itself mounted in the standard specimen adaptor with the stage tilted through 90°, see Figure 2.

To facilitate this arrangement and prevent the stage operating at the end of the Y travel the height-tilt-rotation substage is offset by 35 mm towards the chamber door, a standard procedure on the S250 stage. In this configuration the X, Y and Z movements function in the normal manner with the tilt effectively acting as a height control and the rotate control providing any desired degree of tilt. It has been found in practice that the time taken to switch from the normal mode of operation of the SEM to the CL mode, including the stage modification just described is about 30 minutes.

Since the high collection efficiency of the mirror can only be achieved by its completely surrounding the specimen, other SEM detection modes such as EDX and BSE are excluded. It is, however, possible to obtain emitted electron images using the standard Everhart-Thornley detector, fitted with a short light pipe to prevent fouling of the ellipsoidal mirror. The use of a 'Naton' rather than a phosphor scintillator is also necessary since the latter luminesces very brightly. Images formed using the standard detector in this manner tend to be noisy and have a large backscattered contribution due to generation of secondary electrons at the mirror surface. An improved collection system can be achieved by replacing the standard straight light pipe with a 'swan-necked' pipe to bring the scintillator and cage beneath the edge of the ellipsoidal mirror. The specimen current mode of the SEM remains unaffected, of course, which is useful if it is desired to obtain simultaneous CL and electron beam induced current images.

## The CL detection system

To be generally applicable any CL system is required to operate in three distinct modes : CL spectroscopy, monochromatic imaging and total luminescence imaging. For the first two modes a Spex minimate spectrometer is used, its entrance slit being located at the far focal point of the ellipsoidal mirror. The spectrometer grating has a spectral range from 200-1000 nm, blazed for maximum efficiency at 500 nm. Other gratings can be substituted to extend the spectral range to 40 μm. A range of input and output slits is available to give a spectral resolution ranging from 1 nm to 20 nm. For the highest resolution, narrowest slits, a fibre-optic spot-to-slit converter can be used to improve the optical transfer efficiency. The detector is a Hammamatsu R936 side window photomultiplier tube having a spectral response from 185 to 900 nm. For CL spectra and linescans the use of 'lock-in' amplification gives a significant improvement in signal-to-noise ratio and reduces the effect of stray light. This requires a modulated light input which may be achieved either by blanking of the electron beam or by optical chopping at the monochromator input. The former technique offers better discrimination against background light and permits time resolved studies. The presence of blanking plates in the electron column can, however, compromise the general performance of the SEM and for long persistence luminescence, beam blanking introduces long time constants into the amplification system. For the applications described here optical chopping has proved more convenient although beam blanking is also available. A schematic diagram of the whole collection and detection system is shown in Figure 3.

The requirement for total CL imaging should not be ignored. Not only is it possible to image the whole spectrum of light emitted by the specimen (subject to the constraints of the detector) but the field of view is much greater than that which can be obtained via the monochromator. This is because any optical system which provides a degree of angular compression, as does the ellipsoidal mirror, also magnifies the image by a corresponding amount. The ellipsoidal mirror used in this work magnifies the area of the specimen emitting light by about 18 times at the second focus. For the largest available monochromator slit, 5 mm x 20 mm, this results in a field of view on the specimen of only 1.1 mm x 0.3 mm. The most efficient total CL imaging is achieved by mounting a large area (50 mm diameter) end window PMT directly onto the silica window. This gives a theoretical field of view of ~4.5 mm diameter. It is, however, usually desirable to be able to switch quickly from total CL imaging to monochromatic imaging or spectroscopy. To achieve this a 45° mirror and 34 mm diameter internally silvered hollow light pipe (similar to that described by Boyde and Reid, 1983) is mounted on the front of the monochromator. When moved into the light path this directs virtually all light emitted through the window onto the front end window of a PMT. When moved out of the light path the CL emission is directed into the monochromator. This arrangement gives a theoretical field of view for total CL images of ~3 mm diameter but in practice it is rather larger since the PMT is not at the focal point of the ellipsoidal mirror.

## Applications

### Optical fibre technology

High frequency optical communication over long distances requires very low loss monomode fibres having a high refractive index core a few μm in diameter surrounded by a lower refractive index cladding layer. One method of achieving this is to form successive layers of silica on the inside of a silica glass tube by chemical vapour deposition, doping the innermost layers with germanium to increase the refractive index near the centre. This tube is then collapsed down to form a preform typically 10 mm diameter which may be drawn down to fibres ~150 μm diameter. There is a need to monitor the distribution of the germanium dopant both at the preform stage and in the final fibre. Several techniques such as

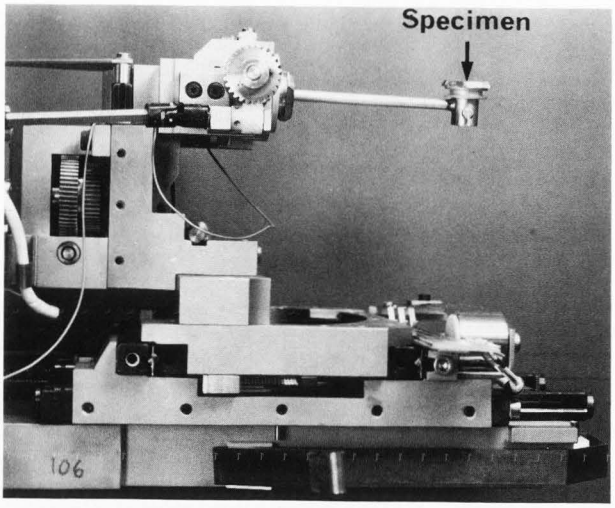


Figure 2 Specimen mounting arrangement for use in CL mode




Figure 3 Schematic diagram of cathodoluminescence system

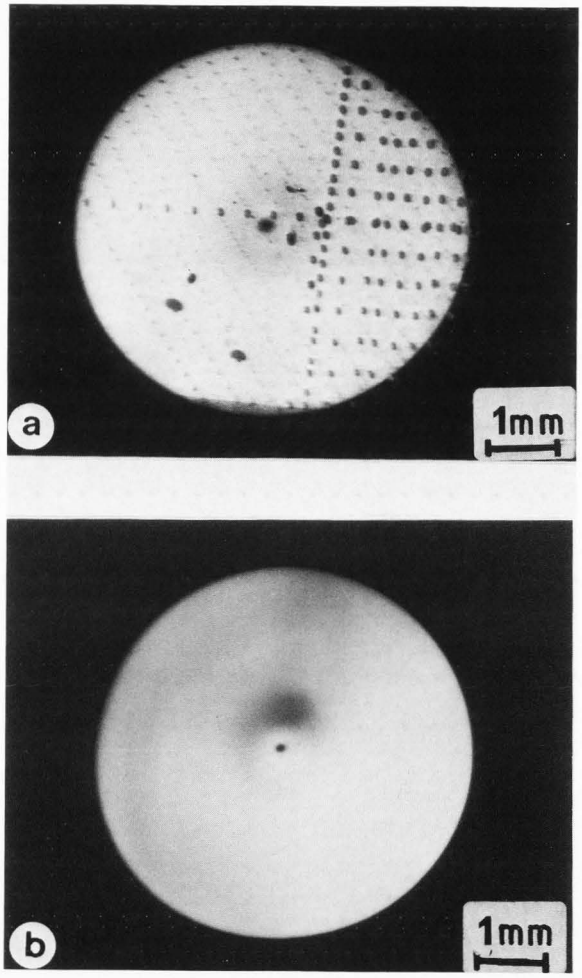


Figure 4 Total CL image of central part of germanium doped optical fibre preform.
(a) After previous EDX point analysis
(b) After repolishing

refractive index measurements, UV excited photoluminescence, energy-dispersive X-ray analysis (EDX) and secondary ion mass spectrometry (SIMS) have been used but only the last two have adequate spatial resolution for studies of the drawn fibres as well as the preforms. Since the germanium concentration is usually only a few percent EDX requires long counting times to achieve adequate signal-to-noise. To obtain a two dimensional map containing 50 x 50 pixels might take several hours. SIMS has much better sensitivity and concentration maps can be obtained quite quickly. Unfortunately, electrostatic charging of the insulating sample can easily lead to irreproducibility.

It is well known that germanium doped silica luminesces under UV excitation at ~400 nm (Presby, 1981a, 1981b) and therefore the possibility of monitoring this emission using cathodoluminescence was investigated. An optical fibre preform whose germanium concentration distribution had previously been studied using EDX was first imaged using total CL. It was observed that there were several superimposed arrays of dark spots where the electron beam had been stationary during EDX analysis, see Figure 4a. These dark areas were not due to electron beam contamination since the original aluminium metallisation, used to prevent electrical charging during the EDX examination, had been stripped off and the sample thoroughly cleaned in isopropyl alcohol prior to subsequent metallisation. It is believed that the dark areas are due to local electron beam reduction of the $SiO_2$:$GeO_2$ (Carriere and Lang, 1977, Remond et al, 1979, and Johannessen et al, 1975). Although the dwell time of the electron beam required either for CL imaging or spectroscopy of the preform was insufficient to cause this effect, it will be seen that electron beam damage can be significant in other forms of silica such as quartz. Prior to further studies the preform was reground and polished; a comparative CL image is shown in Figure 4b, the electron beam damaged areas having been completely removed. Immediately outside the core is the cladding of pure silica from which little luminescence is

emitted. Outside the cladding is the envelope corresponding to the original silica tube; luminescence from this is believed to be related to the presence of impurities such as OH and Al ions (Private communication, J S McCormack). CL spectra from the core and envelope are shown in Figure 5, the germanium doped core region giving a broad luminescence band peaking at 400 nm and the envelope giving a similarly broad band centred at 460 nm.

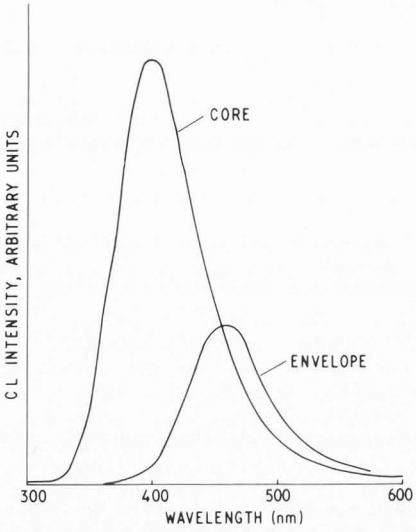


Figure 5 CL spectra from the core and envelope of germanium doped optical fibre preform

Although a qualitative assessment of the germanium distribution can be obtained by CL imaging, a semi-quantitative distribution can be obtained by a CL linescan, see Figures 6a and 6b. It will be observed that there is a sharp dip in CL intensity in the centre of the core with a shoulder on either side. The dip can also be seen as a dark spot at the centre of the core in Figure 4. This results from a reduction in germanium content due to preferential evaporation of germanium oxide from the inside of the tube at the high temperature, 1600-1800°C, required to collapse the tube to form a solid rod. The peaks on either side of the centre-point (arrowed) are due to simultaneous back diffusion of germanium away from the hot tube surface. The asymmetry of the profile in the X direction is due to poor control of the deposition conditions in this, an early prototype preform. Such asymmetry would cause significant optical loss in the final optical fibre.

The CL technique is readily extended to drawn optical fibres and a typical CL image of a cleaved fibre together with a corresponding electron image is shown in Figure 7. This is a multimode fibre in which the relatively large core, ~50 μm diameter, has a graded germanium concentration to give a graded refractive index. Corresponding CL linescans could be obtained in a similar manner as for the preform. In some fibres evidence has been found for the presence of a germanium deficient spot in the centre of the core. The extent of the depletion has not been measured since the diameter

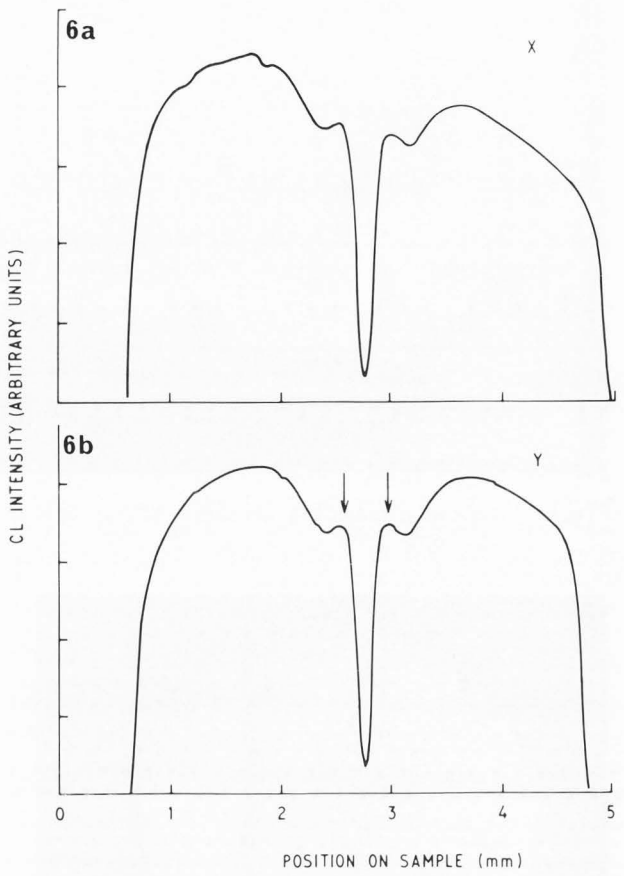


Figure 6 CL linescan across central region of optical fibre preform
(a) In X direction, (b) In Y direction

of the depleted zone is comparable with the spatial resolution of the SEM in the CL mode. This is dominated by electron beam spreading rather than the electron beam spot size and hence the optimum resolution is usually achievable at low accelerating voltages, although at the expense of signal intensity. For optical fibres 5 kV has usually been found most suitable.

Doped synthetic quartz

There have been several previous studies of cathodoluminescence in quartz (Remond et al, 1979, Krinsley and Tovey, 1978 and Grant and White 1978) but these have concentrated mainly on small grains of naturally occurring material rather than large single crystals of controlled doping. More recently Katz et al (1983) have reported cathodoluminescence studies on synthetic quartz which indicated the potential value of the technique.

The synthetic quartz crystals used in this study were grown hydrothermally at ~400°C and 1500 atm from a nutrient of silica in sodium hydroxide. The seed crystals were either high quality natural quartz (Brazilian) or commercially available synthetic quartz.

Although the high quality natural quartz seed crystals appeared to be quite featureless commercial synthetic seeds were not. In one

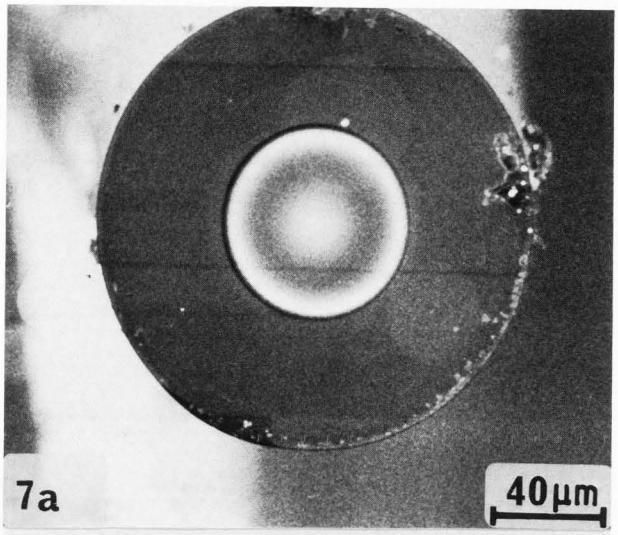


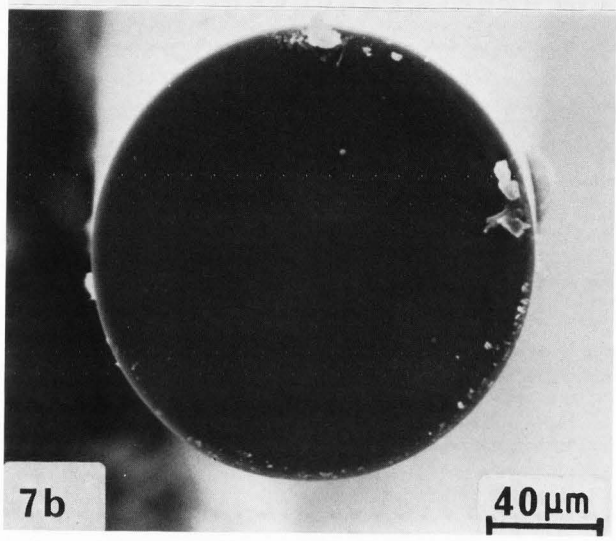


Figure 7 Cleaved multimode optical fibre.
(a) CL image
(b) secondary electron image

sample, a dark striation was observed to run along the whole length ~16 mm of the synthetic quartz seed, see Figure 8. It is an intense growth striation running roughly perpendicular to the Z growth direction and may contain an impurity which kills the luminescence from the quartz, in this instance a broad band centred at 425 nm. The 'scalloped' nature of the growth front is typical of that usually observed in the fast growing Z direction. Higher magnification images revealed that the dark growth striation was actually a doublet comprising a broad striation ~12 µm wide next to a narrower one ~5 µm wide. A regular pattern of much less intense growth striations at ~5 µm intervals was also observed on both sides of the intense band. Assuming that the crystal was grown at a rate typical for commercial crystals of ~0.5 mm per day the striations correspond to ~15 minutes and are probably due to temperature

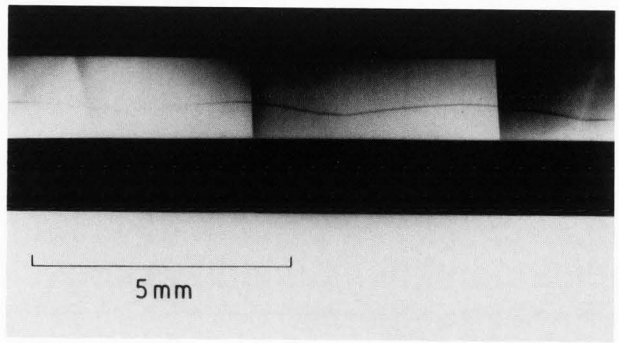


Figure 8 Montage of CL images showing growth striation running along seed crystal

oscillations in the growth furnace. The intense striations must result from a particularly marked temperature excursion.

Doping of synthetic quartz can be achieved by dissolution of the dopant in the nutrient although for most dopants the uptake is very low, <<1%. One dopant which can be introduced quite easily is germanium. Whereas germanium in vitreous silica produces a strong CL emission at ~400 nm this was not observed in quartz. Previous authors (Jones and Embree, 1978) have observed luminescence at 435 nm and 510 nm in germanium doped quartz which also contained other impurities such as aluminium. In the present study, however, the germanium had the effect of shifting the relatively weak 390 nm luminescence band of the undoped quartz to ~480 nm, see Figure 9. Despite the 90 nm peak shift the low intensity and broad band nature of the luminescence preclude the effective use of CL for germanium mapping in quartz, in contrast to its applicability to vitreous silica.

Doping of quartz with aluminium increased the luminescence considerably although uptake of

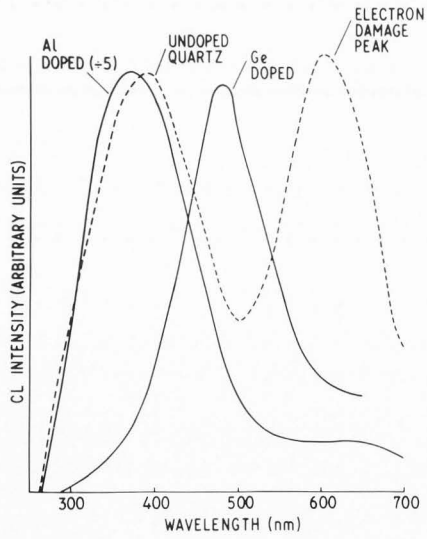


Figure 9 CL spectra of undoped, germanium and aluminium doped quartz

the aluminium was much more pronounced in some crystal growth directions than others. In the fastest growing, Z, direction the concentration of aluminium was found to be 80 ppm, from chemical analysis, and the total CL intensity was approximately the same as that of the seed. The luminescence at the end of the crystal, corresponding to the fast X growth direction was far greater, see Figure 10. Although the luminescence intensity was much higher than that for undoped quartz the CL peak was only slightly displaced by ~30 nm to 360 nm, see Figure 9. The slow X direction, at the opposite end of the crystal also exhibited greatly enhanced luminescence. SIMS studies indicated that the aluminium concentration in the X growth zones was ~370 ppm with up to 650 ppm in the boundary regions between the growth zones. Growth striations are visible in the fast X-fast Z zone boundary region with a periodicity of ~200 μm. Although the Z growth direction material had a generally far lower CL intensity two features are worthy of note. Firstly there is a line of increased emission at the seed-overgrowth boundary, and secondly a large number of bright features extend up to 400 μm into the overgrowth, see Figure 11. All of these bright features originate at irregularities on the seed surface and they probably result from an anomalous crystal growth mechanism leading to a high uptake of aluminium. Further studies of these features are currently being undertaken using X-ray topography.

Bismuth silicon oxide

There is at present considerable interest in the use of degenerate four wave mixing (DFWM) for real-time optical processing (Laycock and Petts, 1983, Laycock et al, 1984). DFWM is an optical phenomenon in which a grating structure is formed in a non-linear medium, usually a photorefractive crystal, by the interaction of two input waves. The third input wave can be considered as diffracting from the induced grating giving rise to the fourth, output wave. The successful implementation of DFWM depends largely on obtaining suitable photorefractive crystals of convenient size, optical quality and damage threshold. At present bismuth silicon oxide, $Bi_{12}SiO_{20}$ (BSO) is proving most suitable and hence the growth of large, high quality crystals is necessary. Czochralski growth from the melt at 925°C has proved most successful in producing crystals up to 20 mm diameter.

Good optical quality and a high laser damage threshold require a low concentration of imperfections in the crystal and hence the CL technique was evaluated to ascertain whether it could yield useful information on this aspect of crystal growth. It was found that BSO exhibited a fairly weak, broad CL band at ~350 nm, see Figure 12. On the macroscopic scale cross-sections of a BSO crystal were quite featureless but at higher magnifications circular growth striations were clearly visible at ~7 μm intervals. These are due to local temperature fluctuations as the crystal boule is rotated in the melt since the centre of rotation does not coincide exactly with the thermal axis of the melt. Since the boule is rotated at 8 revolutions per minute and assuming that each striation corresponds to one rotation the outward growth rate can be calculated to be 3.3 mm per hour, compared with the vertical growth rate of 1 mm per hour.

As well as quartz and BSO a number of synthetic crystals of optically important materials such as doped yttrium aluminium garnet (YAG), polycrystalline zinc selenide (Russell et al 1981), and potassium tantalum niobate have been usefully studied in these laboratories using the CL technique. For example it has proved valuable in monitoring the variability of crystal strain in neodymium-doped YAG due to slight fluctuations of temperature at the growth front as a function of time. Figure 13 is a total CL image of a cross-section through one such crystal which shows clearly the striations associated with growth both along the axis of the boule and outward from it.

## Summary

A high efficiency versatile spectroscopic CL system has been built which can be easily fitted to an existing standard SEM. Although as currently configured the system operates in the 200-900 nm region of the spectrum, it can be readily extended to longer wavelengths. For semiconductor materials in particular it is well established (Holt and Datta 1980, Cumberbatch et al 1981) that reducing the sample temperature enhances the spectral resolution and increases luminescent intensity by reducing the probability of competing non-radiative recombination. For this reason most semiconductor photoluminescence studies are carried out at ~4.2K (Bishop 1981). Designs for a cooling facility suitable for the cathodoluminescence system described here are currently being considered but it is unlikely that specimen temperatures much below ~80K will be achieved because of the mechanical constraints of the specimen stage.

The interpretation of CL spectra and images is far from trivial and the need for parallel studies using other techniques such as EDX, SIMS and X-ray diffraction etc., cannot be over-emphasised. One of the great advantages of CL, in common with many other modes of the SEM, is its ability to provide information in real-time. Thus although X-ray topography may ultimately be a more powerful tool for the study of imperfections in quartz, for example, a single exposure requires several hours (and may then need to be repeated). A CL image on the other hand can be obtained in ~2 minutes and immediately provides useful information on the quality of the crystal. The system described here has proved very valuable for the study of optical materials such as germanium doped silica and synthetic quartz. In the latter material CL has revealed several unexpected features some of whose origins are still being investigated.

## Acknowledgements

The author is indebted to many of his colleagues at Hirst Research Centre for their help and encouragement during this work. In particular thanks are due to Dr J McCormack, Mr J A James and Mr D F Croxall who provided the

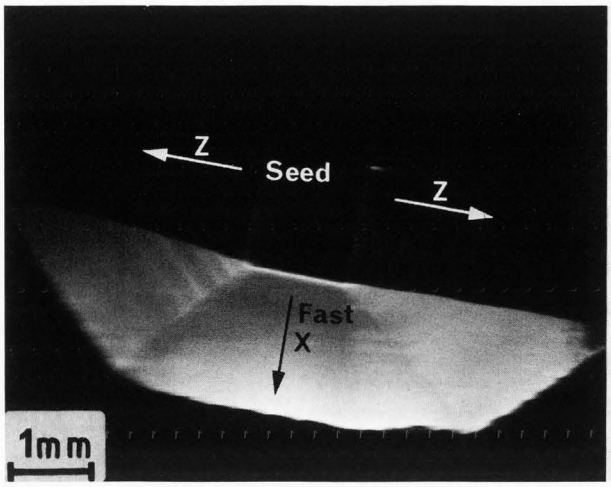


Figure 10 Total CL image of end of aluminium doped quartz crystal. Arrows refer to crystal growth directions

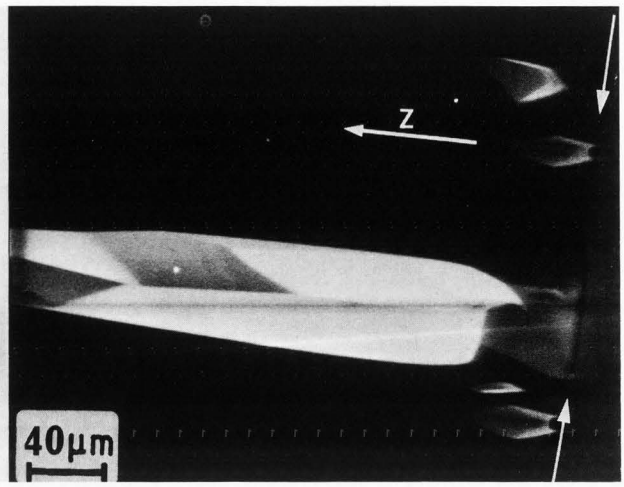


Figure 11 Total CL image of bright features 'growing' from seed-overgrowth interface (arrowed). Z refers to growth direction

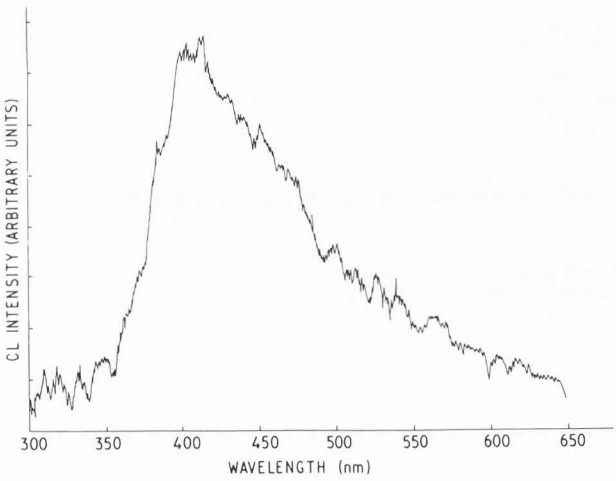


Figure 12 CL spectrum of bismuth silicon oxide

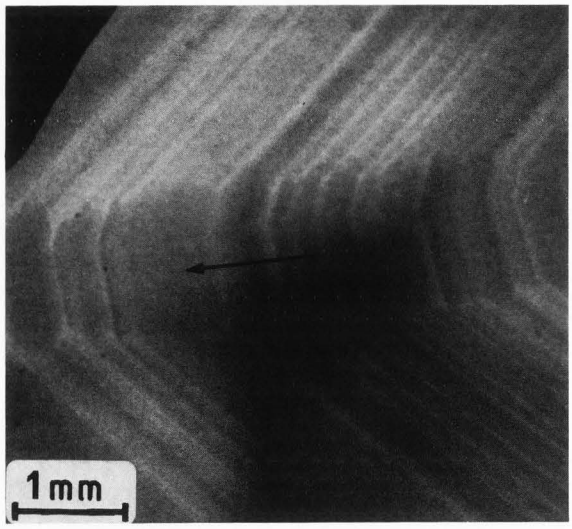


Figure 13 CL image of neodymium doped YAG crystal showing growth striations. Arrow marks growth axis of crystal

samples without which the work would not have been possible.

References

Beavineau J, Semo J. (1982). Improved spectrometer for cathodoluminescence studies in scanning electron microscopy. Rev Sci Instrum 53(10), 1573-1576.

Bishop SG. (1981). Characterisation of semiconductors by photoluminescence and photoluminescence excitation spectroscopy. Proceedings of the International Society for Optical Engineering, Bellingham, VA 98227-0010, Vol. 276, 2-10.

Boyde A, Reid SA. (1983). New methods for cathodoluminescence in the scanning electron microscope. Scanning Electron Microsc. 1983; IV: 1803-1814.

Brocker W, Pfefferkorn G. (1978). A bibliography of cathodoluminescence. Scanning Electron Microsc. 1978; I: 333-351.

Brocker W, Pfefferkorn G. (1980). A bibliography of cathodoluminescence Part II. Scanning Electron Microsc. 1980; I: 298-302.

Carlsson L, Van Essen CG. (1974). An efficient apparatus for studying cathodoluminescence in the scanning electron microscope. Journal of Physics E: Scientific Instruments 7, 98-100.

Carriere B, Lang B. (1977). A study of the charging and dissociation of $SiO_2$ surfaces by AES. Surface Science 64, 209-223.

Chin AK, Caruso R, Young MSS, Von Neida AR. (1984). Uniformity characterisation of semi-insulating GaAs by cathodoluminescence imaging. Appl Phys Lett 45(5), 552-554.

*Cumberbatch TJ, Davidson SM, Myhajlenko S. (1981). Cathodoluminescence imaging of silicon. Inst Phys Conf Ser No 60(4), 197-202.

Davidson SM, Barnes SC, Rasul A. (1976). A scanning electron microscope for semiconductor studies. Developments in electron microscopy and analysis: Academic Press, London 105-110.

*Davidson SM, Cumberbatch TJ, Huang E, Myhajlenko S. (1981). A new scanning cathodoluminescence microprobe system. Inst Phys Conf Ser No 60(4), 191-196.

Davidson SM, Rasul A. (1977). A high resolution cathodoluminescence analysis system. Journal of Physics E: Scientific Instruments 10, 43-46.

Grant PR, White SH. (1978). Cathodoluminescence and microstructure of quartz overgrowths on quartz. Scanning Electron Microsc. 1978; I: 789-793.

*Holt DB. (1981). Recent developments in SEM detection systems for the cathodoluminescence and conductive modes. Inst Phys Conf Ser No 60(4), 165-178.

Holt DB, Datta S. (1980). The cathodoluminescence mode as an analytical technique: its development and prospects. Scanning Electron Microsc. 1980; I: 259-278.

Holt DB, Steyn JB, Giles P. (1976). Spectroscopic cathodoluminescence mode scanning electron microscopy. Developments in electron microscopy and analysis. Academic Press, London, 111-114.

Hörl EM. (1978). Cathodoluminescence : actual state of instrumentation. Microscopica Acta Suppl 2 Microprobe analysis in Biology and Medicine, 236-248.

Hörl EM. (1972). Scanning electron microscopy of biological material using cathodoluminescence. Micron 3, 540-544.

Johannessen JS, Spicer WE, Strausser YE. (1975). Phase separation in silicon oxides as seen by Auger electron spectroscopy. Appl Phys Lett 27(8), 452-454.

Jones CE, Embree D. (1978). Cathodoluminescence studies of $SiO_2$ -Na, Cl, Ge, Cu, Au and oxygen vacancy results. The Physics of $SiO_2$ and its interfaces: (ed) S T Pantelides Pergamon Press, Oxford, 289-293.

Katz S, Halperin A, Schieber M. (1983). Characterisation of quartz crystals by cathodoluminescence. Proceedings of the 37th Annual Frequency Control Symp. IEEE, NY 185-186.

Krinsley D, Tovey NK. (1978). Cathodoluminescence in quartz sand grains: Scanning Electron Microsc. 1978; I: 887-894.

Laycock LC, McCall MW, Petts CR. (1984). A compact real-time optical processing system. GEC Journal of Research 2(2), 82-87.

Laycock LC, Petts CR. (1983). Two dimensional optical image processing for pattern recognition. GEC Journal of Research 1(2), 127-135.

*Löhnert K, Hastenrath M, Balk LJ, Kubalek E. (1981). A scanning electron microscope based cathodoluminescence measurement system instrumentation and capabilities. Inst Phys Conf Ser No 60(4), 179-184.

*Löhnert K, Kubalek E. (1983). Characterisation of semiconducting materials and devices by EBIC and CL techniques. Inst Phys Conf Ser No 67(6), 303-314.

Presby HM. (1981a). Fluorescence profiling of single mode optical fibre preforms. Applied Optics 20(3), 445-450.

Presby HM. (1981b). Ultraviolet-excited fluorescence in optical fibres and preforms. Applied Optics 20(4), 701-706.

Remond G, LeGressus C, Okuzumi H. (1979). Electron beam effects observed in cathodoluminescence and Auger electron spectroscopy in natural materials : Evidence for ionic diffusion. Scanning Electron Microsc. 1979; I: 237-244.

Richards BP, Trigg AD, King WG. (1983). Investigation of fluorescent lamp phosphors using the combined CL and EDS modes of the SEM. Scanning 6, 8-19.

*Russell GJ, Waite P, Woods J, Lewis KL. (1981). Electrically active grain boundaries in polycrystalline zinc selenide: Inst Phys Conf Ser 60(7), 371-376.

Steyn JB, Giles P, Holt DB. (1976). An efficient spectroscopic detection system for cathodoluminescence mode scanning electron microscopy (SEM). J. Microscopy 197(2) 107-128.

*Published by The Institute of Physics, Bristol and London.

## Discussion with Reviewers

E M Hörl: Discussing the efficiency of your CL system it should be mentioned that an appreciable fraction of the CL light emitted by the specimen is lost by the fact that the specimen and its supporting rod shields off part of the beam reflected by the mirror. This loss in CL intensity is even more to consider since CL emission is strong in directions nearly perpendicular to the specimen surface. What fraction of total intensity do you think you lose in this way?
Author: For a specimen stub of 8 mm diameter the loss in intensity caused by the specimen and support rod obscuring light reflected from the mirror is ~6% if the light is emitted uniformly over a complete hemisphere or ~15% if the angular dependence of emission follows a cosine distribution.

D B Holt: Your point that elliptical mirrors provide magnification and limit the field of view is important. The severe limitation you quote is apparently due to the large ellipticity of your mirror. Can you indicate the range of values of field of view that would arise for different ratios of the major and minor axes?
Author: The field of view depends not only on the ellipticity of the mirror but also on the spectral resolution required or, for total CL, the area of the detector. For the 20 mm x 5 mm slit on our monochromator, corresponding to 20 nm resolution, the field of view would increase from 1.1 mm x 0.3 mm for our 18:1 ellipticity mirror to 4 mm x 1 mm for a 5:1 mirror. A lower ellipticity than this would almost certainly bring the second focus inside the vacuum chamber negating many of the advantages of this approach.

G Koschek: What are the advantages of your system compared to the CL equipment as described by Löhnert et al (1981 text reference) except that it seems to be easily removable from the SEM?
Author: Löhnert's system as described in the above paper falls into the category of expensive CL systems which require an SEM to be dedicated to CL studies. I do not believe therefore that a direct comparison with our system is valid. There is, however, no reason why a system based on Löhnert's design could not be easily removable from the SEM. In terms of collection efficiency our system is about a factor of 3 higher because of the higher solid angle subtended by the mirror.

G Koschek: Your CL micrographs are not examples of high spatial resolution. Please give a concrete value for the spatial resolution obtainable on optical fibres.
Author: For materials which are transparent to their own luminescence, such as optical fibres, the spatial resolution in the CL mode is limited by electron beam spreading in the sample. Reducing the electron beam energy enhances the spatial resolution while reducing the total CL intensity. At a beam voltage of 5 kV we achieve a spatial resolution of 0.5 μm.

G Koschek: How is the spatial resolution of the 'unmodified' SEM affected by adaptation of the CL stage? How is the electron collection efficiency (SE/BSE-mode) changed by use of the new electron collection system (scintillator, light pipe)?
Author: In principle the spatial resolution of the SEM is not affected at all. But the new electron collection system has a much lower efficiency, ~1.6% compared to the original one since it is not in the line of sight of the specimen. In practice this reduces the effective resolution that can be obtained to ~25 nm instead of the 5 nm achievable with the SEM as normally configured. This is of little consequence since for CL high electron beam currents are usually required and the resolution is limited by beam spreading rather than the diameter of the electron beam.

R C Farrow: How much improvement would you expect in the sharpness of CL spectral lines if you were to cool the sample down to liquid helium temperature?
Author: For semiconductors a significant improvement in spectral resolution would be expected. In ZnS for example the full width at half maximum (FWHM) of the 340 nm edge emission falls from ~6 nm at 280K to ~2 nm at 76K (Roberts SH, Steeds JW, 1982, High resolution in scanning cathodoluminescence of ZnS edge emission, J. Crystal Growth, 59, 312-316). In silicon the FWHM falls from ~140 nm at 300K to ~13 nm at 16K (Cumberbatch et al 1981 text reference). For insulating materials such as quartz the situation is less clear with broad bands having an FWHM of 190 nm being observed even at 4.2K (Grinfelds et al 1984, Low temperature recombination luminescence in amorphous and crystalline $SiO_2$, Physica Status Solidi (a) 81 K23-K26).

G Koschek: How do you intend to install a cold stage on your CL equipment?
Author: The sample would be thermally coupled to a liquid nitrogen reservoir via a flexible copper braid. A similar approach has been used by Davidson et al (1981 text reference) and has achieved temperatures down to 10K using a liquid helium cryostat.

D B Holt: The form of beam damage you report in silica-germania mixtures is worrisome. Can you give any indication of the threshold dose for this damage? Does anything equivalent occur in silica?
Author: There does not appear to be any specific damage threshold but for germanium doped silica no obvious degradation was observed with a dose of $10^{-2}$C cm$^{-2}$ at 20 kV. Similar effects are observed in both vitreous silica and quartz. The latter material is more susceptible to electron beam damage and degradation was apparent after a dose of only $10^{-4}$C cm$^{-2}$.

E M Hörl: Are there currently any ideas on:
(1) Where the germanium atoms are located in the silica lattice and where the germanium or aluminium atoms are located in the quartz lattice?

(2) What the crystal field around such an impurity atom looks like?
(3) What kind of new energy levels are expected?
(4) What kind of CL emission spectra one should observe from a theoretical point of view?

Author: It is generally believed that the germanium may either substitute for the silicon as $GeO_2$ or may exist in the form GeO; there is evidence that this latter species is responsible for the observed luminescence (Philen DL and Anderson WT, 1982. Analysis of the fluorescence method of profiling single-mode optical fibre preforms, Digest of Technical Papers of the 5th Topical Meeting on Optical Communication, Phoenix, Arizona, p 66). In quartz both germanium and aluminium substitute for the silicon, the aluminium usually being associated with a charge compensating alkali ion. It is believed that it is this Al-$M^+$ centre which is responsible for the luminescence observed from aluminium doped quartz (Katz et al 1983, text reference).
In answer to the subsequent parts of your question I would refer you to Robertson J, (1982) Atomic defects in glasses, Physics and Chemistry of glasses, 23 1-17.

G Koschek: Can you comment on how far a fibre optic spot to slit converter can improve the optical signal intensity?
Author: A spot to slit converter can improve the optical coupling to the spectrometer by a factor of up to 2.9.

E M Hörl: How are backscattered electrons prevented from hitting the silica window where they cause unwanted secondary CL? Can this secondary CL be separated from the primary one? How high is its contribution to the background noise?
Author: Any electrons backscattered from the sample strike the ellipsoidal mirror, they cannot directly strike the silica window and no luminescence has been observed from it. Luminescence from the epoxy ellipsoidal mirror can occur if the aluminium coating is insufficiently thick or has pin-holes in it. This luminescence would not of course be brought to focus at the monochromator slit with the true specimen cathodoluminescence and no background contribution from it has been observed.